Estimating tree species diversity from space in an alpine conifer forest: the Rao's Q diversity index meets the Spectral Variation Hypothesis

Michele Torresani [1*], Duccio Rocchini[2,3,4], Ruth Sonnenschein[5], Marc Zebisch[5], Matteo Marcantonio[6], Carlo Ricotta[7], Giustino Tonon[1]

November 22, 2019

[1] Free University of Bolzano/Bozen, Faculty of Science and Technology, Piazza Universitá / Universitätsplatz 1, 39100, Bolzano/Bozen, Italy

[2] University of Trento, Center Agriculture Food Environment (C3A), Via E. Mach 1, 38010 S. Michele all'Adige (TN), Italy

[3] University of Trento, Department of Cellular, Computational and Integrative Biology (CIBIO), Via Sommarive, 14, 38123 Povo (TN), Italy

[4] Fondazione Edmund Mach, Research and Innovation Centre, Department of Biodiversity and Molecular Ecology, Via E. Mach 1, 38010 S. Michele all'Adige (TN), Italy

[5] Institute for Earth Observation, EURAC, European Academy of Bolzano/Bozen, Viale Druso 1, Bolzano/Bozen, Italy

[6] Department of Pathology, Microbiology, and Immunology, School of Veterinary Medicine, University of California, Davis, USA

[7] Department of Environmental Biology, University of Rome "La Sapienza", Rome 00185, Italy

* corresponding author: michele.torresani@natec.unibz.it

Abstract

Forests cover about 30% of the Earth surface, they are among the most biodiverse terrestrial ecosystems and represent the bulk of many ecological processes and services. The assessment of biodiversity is an important and essential goal to achieve but it can results difficult, time consuming and expensive when based on field data. Remote sensing covers large areas and provides consistent quality and standardized data, which can be used to estimate species diversity. One method to estimate species diversity from remote sensing data is based on the Spectral Variation Hypothesis (SVH), which assumes that the higher the spectral variation of an image, the higher the environmental heterogeneity and the species diversity of the considered area. SVH has been tested using different spectral heterogeneity (SH) indices and measures, recently the Rao's Q index has been proposed as a new spectral variation measure to be applied to remote sensing data. In this paper, we tested the SVH in an alpine coniferous forest to estimate tree species diversity. We evaluated the performance of the Rao's Q index and compared it with another widely used SH index, the Coefficient of Variation (CV), validating them against values of Shannon's H (used as species diversity index) derived from in-situ collected data. A NDVI time-series (for 2016 and 2017) derived from the Sentinel-2A and 2B and Landsat 8 OLI satellites has been used to test the effect of the spatial grain of both the sensors and to understand the seasonality of the SVH. The results showed that the SVH is season and sensor dependent. For both years and satellites, the relation between Rao's Q and field data reached the highest R^2 between June and July, decreasing towards winter and spring similarly to the NDVI time-series. This relationship could be given because, when NDVI reaches its highest values, it is able to capture small variation in reflectance of different leaf traits typical of specific trees. The relation between field and spectral diversity reached a value of R^2=0.70 (2017) and R^2=0.48 (2016) for Sentinel-2 and of R^2=0.42 (2017) and R^2=0.47 (2016) for Landsat 8. CV showed the same NDVI temporal tendency. However, the relation between field-derived Shannon's H and CV was on average lower than that we found for Rao's Q. This research underlined the goodness of the Rao's Q index, the relevance of the NDVI in the study of the SVH and the importance of the multi-temporal approach.

Keywords: alpine ecosystems, biodiversity, environmental heterogeneity, spectral heterogeneity index, remote sensing, time series analysis.

1 Introduction

1.1 Forest biodiversity and remote sensing

Forest biodiversity is the variability among living organisms in forest ecosystems encompassing the diversity of species across forest ecosystems (Whittaker, 1960). It also accounts for the ecological structures, functions and processes in forest ecosystems (Kaennel, 1998), (Innes and Koch, 1998) which play a key role for human well-being. Forests cover approximately 30% of the Earth's land surface (Mace et al., 2012) and provide food, medicines, fuel and other necessities to approximately 1.6 billion people. They support water flow regulation, carbon storage, and services such as habitat preservation (Team et al., 2007), pollution control (Grote et al., 2016), and soil protection and formation (Cunningham, 1963).

Many of the essential benefits deriving from forests depends on their biodiversity (Fleming et al., 2011). Forests are among the most biodiverse terrestrial ecosystems, they have the highest species diversity for many taxonomic groups, and they support about 65 % of the world's terrestrial taxa hosting two-thirds of all plants and animals living on land. (Lindenmayer et al., 2006). Although the importance of biodiversity is well known (Gamfeldt et al., 2008), forest biodiversity is declining due to a series of causes including habitat degradation (Hanski, 2011), unsustainable forest management (Chaudhary et al., 2016), climate change (Bellard et al., 2012), and pollution (McNeely et al., 1992) worldwide.

In the 1960s, Whittaker (Whittaker, 1960) introduced the terms of alpha, beta and gamma biodiversity to measure diversity at different spatial scales. Alpha biodiversity represents the species diversity within a specific area or ecosystem and can be expressed by the number of species (i.e., species richness). However, diversity indices, that also take into account the abundances of species (evenness), such as the Shannon's diversity index (H) (Shannon, 1948) are more widely used (Oldeland et al., 2010), (Nagendra , 2002), (Gorelick et al., 2006).

Species diversity can be directly assessed through field sampling. However, for large areas, this can be costly and time consuming. Therefore, efficient methodologies and tools that estimate species diversity and the related human impact are needed (Nagendra , 2001). Earth observation is a key instrument for monitoring ecosystems and the recent advances in sensor technology (high spatial resolution, broad coverage and high revisit frequency) make its application in highly heterogeneous ecosystems possible and economically acceptable. The assessment of forest biodiversity has been accomplished using different remote sensing data (Nagendra et al., 2010).

For instance, active sensors like LiDAR (Light Detection and Ranging) and radar have been used to evaluate the relationship between 3D structure and vegetation species diversity (Bergen et al., 2009), (Simonson et al., 2012) and animal richness (Muller et al., 2009), (Jung et al., 2012), (Muller et al., 2014). Optical images have been also largely used for this purpose. Digital Aerial photographs have been used to map tropical (Garzon-Lopez et al., 2013) and temperate (Getzin et al., 2012) forests. Hyperspectral images showed excellent results to map some aspects of biodiversity in different forest ecosystems, including tropical (Laurin et al., 2014), rain (Carlson et al., 2007), conifer (Gong et al., 1997) and mixed mountain forests (Schneider et al., 2017) . Multi-spectral data from unmanned aerial vehicles (UAV) (Dandois et al., 2015), airborne (Lassau et al., 2005) and from satellite (Rocchini, 2007), (Nagendra and Rocchini, 2008) provided also very interesting results for the assessment of some aspects of forest biodiversity. In this context, the recently launched Sentinel-2 mission, which was developed by the European Space Agency (ESA) as part of the Copernicus program is fundamental with its free and open data access policy. This mission consists of a constellation of two optical satellites (Sentinel-2A and Sentinel-2B) that acquire images with 13 spectral bands (with resolution between 10 and 60 meters) and a revisit frequency of 5 days (at equator). Sentinel-2 has shown promising results in the monitoring of forest ecosystems, in tree species classifications (Immitzer et al., 2016), forest mapping (Puletti et al., 2017), monitoring forest disturbances (Verhegghen et al., 2016) and predicting growing stock volume (Mura et al., 2018), (Chrysafis et al., 2017).

Furthermore, the use of remote sensing data to measure some aspects of biodiversity has been increasingly considered as an elective choice of many worldwide initiatives (Rocchini et al., 2018). In particular the Group on Earth Observations - Biodiversity Observation Network - GEO BON (`www.geobon.org`) developed the concept of essential biodiversity variable (EBV), a *"derived measurement required to study, report, and manage biodiversity change, focusing on status and trend in elements of biodiversity"* that can be easily defined through satellite information (Jetz et al., 2016).

1.2 The Spectral Variation Hypothesis and the Rao's Q index

Remote sensing data can be used to assess certain aspect of biodiversity through direct and indirect approaches (Turner et al., 2003). Direct approaches require data with high spatial or spectral resolution and aim to map targets (individual species or communities) directly from remote sensing data

(Write et al., 2010). Indirect approaches can be of two types (Nagendra , 2001). In the first type, environmental characteristics are derived from remotely sensed data that are then used to generate species distribution maps based on a priori knowledge (Gillespie et al., 2008). In the second type, direct relationships between remotely sensed reflectance values and field-based data of species diversity are produced (Palmer et al., 2002).

An example of the latest approach is based on the Spectral Variation Hypothesis (SVH) proposed for the first time by Palmer et al. (2002). This concept hypothesizes that the variability of the spectral response of a remotely sensed image could be used as a proxy to assess plant biodiversity. Areas with high spectral heterogeneity (SH) in a remotely sensed image correspond to a higher number of available ecological niches that can host more species. Therefore, the spectral variation of an image is related to the environmental heterogeneity and could be used as a powerful proxy of species diversity (Palmer et al., 2002).

The SVH has been tested in different ecosystems including wetlands (Rocchini et al., 2017), prairie vegetation (Palmer et al., 2002), tropical forests (Féret and Asner, 2014), grasslands (Lopes et al., 2017) and Mediterranean vegetation (Levin et al., 2007). Recently Schmidtlein and Fassnach (Schmidtlein and Fassnacht, 2017) tested the SVH across different habitats observing that it does not hold across different ecosystems, stressing its ecosystem dependency. The SVH has been tested using data from airborne hyperspectral sensors (Oldeland et al., 2010), (Gholizadeh et al., 2018), multi-spectral satellite such as MODIS (Schmidtlein and Fassnacht, 2017), Landsat (Rocchini, 2007), (Levin et al., 2007), QuickBird (Hall et al., 2010), ASTER (Levin et al., 2007) and SPOT (Lopes et al., 2017). These studies showed the strong sensor dependency of SVH resulting from different spatial scales (spatial resolution and image extent) and spectral scales (number of bands, radiometric resolution, band width and spectral range covered).

SVH also strongly depends on the index used to calculate the SH. Some indices like the convex hull volume and convex hull area (Gholizadeh et al., 2018) require a multi-dimensional image. Other indices like the coefficient of variation (CV) can be derived from a single band (Madonsela et al., 2017) or from spectral indices, such as the Normalized Difference Vegetation Index (NDVI) (Tucker, C. J., 1979), (Oindo and Skidmore, 2002), (Levin et al., 2007), (Gould et al., 2000).

Recently the Rao's Q index has been proposed as an innovative SH measure in the field of remote sensing (Rocchini et al., 2017). The Rao's Q index has been developed by Rao (Rao, 1982), and proposed by Botta-Dukat (2005) as a measure of functional diversity in ecology. As stated by Rocchini et al. (2017) "given an image of N pixels, the Rao's Q is related to the sum

of all the pixel values pairwise distances, each of which is multiplied by the relative abundance of each pair of pixels in the analyzed image. Rao's Q is the expected difference in reflectance values between two pixels drawn randomly with replacement from the considered evaluated pixels set." Hence, Rao's Q considers both the value of the pixel (through the distance/difference between the pixel) and the abundance of the pixel in the image.

The aim of this paper is to test the Spectral Variation Hypothesis in an alpine coniferous forest to estimate tree species diversity. In particular the objective of this research is to evaluate the performance of the Rao's Q, comparing it with the CV (used as a benchmark) and to validate them against values of Shannon's H (used as species diversity index) derived from in-situ collected data. The SVH has been tested using an NDVI data-set derived from Sentinel-2 and Landsat 8 for the year 2016 and 2017. This has been done to test the effect of the spatial grain of different sensors and to understand the seasonality of the SVH.

2 Material and methods

2.1 Field data

The study area is located in a coniferous forest at 1100 m a.s.l. in the municipality of San Genesio/Jenesien, in South Tyrol (Italy, Figure 1). The dominant species is *Pinus sylvestris*, followed by *Larix decidua* and *Picea abies* while broadleaved trees such as *Betula alba*, *Corylus avellana*, *Salix caprea* and *Sorbus aucuparia* are accessory species. The forest is particularly dense and characterized by a high canopy closure. We chose a coniferous forest since SVH has never been tested in such ecosystems. Furthermore, the considered area has a particular species diversity gradient, with regions where the overall species diversity is very low (pure pine forest) and areas with a higher mixture of different tree species.
Twenty squared study plots were randomly placed within the forest, with a size for each plot of 1 ha (100m x 100m) defined following similar sampling designs (Schmidtlein and Fassnacht, 2017), (Rocchini, 2007), (Oldeland et al., 2010). The field campaign was carried out in summer 2017. All plots were geo-referenced with a GPS device (spatial accuracy $\pm 3m$) to obtain the exact position of the center and the four corners. Trees with a diameter at breast high (DBH) of at least 5 cm were classified by species. The number of individuals per plot ranged from 466 to 3196 (with a total amount of sampled individuals corresponding to 19827), attaining to a number of species ranging from 4 to 11.

Due to the low amount of species (total amount = 15 species) expected in this type of habitat (Gong et al., 1997), we decided to rely on the Shannon's H index (Equation 1) as a measure of species diversity calculated for each plot, starting from the sampled individuals. Shannon's H is one of the most frequently used ecological index, it is sensitive to both rarity and species abundance and has been used in different studies as a measure of alpha diversity (Madonsela et al., 2017), (Oldeland et al., 2010). Strictly speaking, making use of abundance based measures is expected to improve models of species versus spectral diversity (Oldeland et al., 2010).

$$H_e = -\sum_{i=1}^{n} p_i * ln(p_i) \tag{1}$$

where:

H_e = Shannon's entropy used in ecology

n = total number of individuals

p = proportion of individuals attaining to species i relative to the total number of individuals

2.2 Remote sensing data

The SVH has been tested using NDVI time-series derived from Sentinel-2 and Landsat 8 OLI for the years 2016 and 2017. The choice to use NDVI has been based on the assumption of previous studies (Madonsela et al., 2017), (Gillespie, 2005), (Parviainen et al., 2010) that variability in NDVI is related to species diversity. NDVI is one of the most widely used remote-sensing based vegetation indices to quantify the biomass of an ecosystem. NDVI derived from remotely sensed observations is related to the energy exchanged in an ecosystem and with primary productivity (Parviainen et al., 2010). Such relation has been found to be a valid indicator of regional variation in species diversity. Furthermore we hypothesize that the small variation in reflectance of different leaf traits, typical of specific trees can be captured by NDVI (He et al., 2009). All images with the lowest amount of noise (e.g., snow, shadows, clouds, aerosols) were used for this purpose (Appendix 1). Sentinel-2A and 2B satellite images (Level-1C) acquired with the relative orbit numbers R022 and R065 and provided as 32TPS were downloaded from the ESA's Sentinel Scientific Data Hub. The Landsat 8 images (Level-1TP) with a Worldwide Reference System (WRS) path of 192 and 193, and WRS row of 027 and 028 were obtained from the Earth Explorer Hub of the

USGS. Both products were radiometrically calibrated and orthorectified by the providers using ground control points and digital elevation models. Due to the different radiometric data formats, we converted Landsat OLI Digital Numbers (DNs) to top of atmosphere (TOA) reflectance (Equation 2) to allow comparability with the Sentinel-2 Level-1C data format (Bhardwaj et al., 2015) .

$$\rho_\lambda = \frac{M_\rho Q_{cal} + A_\rho}{cos(\theta_{SZ})} \tag{2}$$

where:

ρ_λ = TOA reflectance

M_ρ = band-specific multiplicative rescaling factor

Q_{cal} = quantized and calibrated standard product pixel values

A_ρ = band-specific additive rescaling factor from the metadata

$cos(\theta_{SZ})$ = cosine of local solar zenith angle

NDVI was derived for both sources of images, following the standard formula:

$$NDVI = \frac{NIR - RED}{NIR + RED} \tag{3}$$

where:

NIR = Near Infrared band

RED = Red band

NIR 8th and 5th band were used for the Sentinel-2 and Landsat 8 respectively, and RED 4th band was used for both the satellites. The spatial resolution of bands 4 and 8 of Sentinel-2 was 10 m, while the spatial resolution of band 4 and 5 of Landsat 8 was 30m. The derived NDVI had then a spatial resolution of 10 and 30 m respectively for Sentinel-2 and Landsat 8.

2.3 Spectral heterogeneity indices

The SH was calculated for all 20 plots for all images and for both satellites using the derived NDVI images. Two indices were used to calculate the SH: the Rao's Q and the Coefficient of Variation (CV).

The Rao's Q diversity index (Rao, 1982) was proposed by Botta-Dukat (2005) as a measure of functional diversity in Ecology with the following formula:

$$Q_e = \sum_{i=1}^{C-1} \sum_{j=i+1}^{C} d_{ij} * p_i * p_j \tag{4}$$

where:

Q_e = Rao's Q used in ecology

p = relative abundance of a species in a community (C)

d_{ij} = distance between the i-th and j-th species ($d_{ij} = d_{ji}$ and $d_{ii} = 0$)

i = species i

j = species j

Botta-Dukat (2005) proposed that d_{ij} can be calculated considering the differences in character/traits of the considered species, using different distance functions (Legendre and Legendre, 1998), (Podani et al., 2000) such as the Euclidean distance divided by the number of the traits/characters:

$$d_{ij} = \frac{1}{n} \sum_{k=1}^{n} (X_{ik} - X_{jk})^2 \tag{5}$$

or the mean character difference:

$$d_{ij} = \frac{1}{n} \sum_{k=1}^{n} |X_{ik} - X_{jk}| \tag{6}$$

where:

n = number of traits considered

X_{ik} = value of trait k in species i

X_{jk} = value of trait k in species j

Rocchini et al. (2017) applied the Rao's Q index to optical remote sensing data, as SH measure, using the distance d_{ij} among pixel values of an image, and their relative abundance, calculated as:

$$Q_{rs} = \sum_{i=1}^{F-1} \sum_{j=i+1}^{F} d_{ij} * p_i * p_j \tag{7}$$

where:

Q_{rs} = Rao's Q applied to remote sensing

p = relative abundance of a pixel value in a selected plot image (F)

d_{ij} = spectral distance between the i-th and j-th pixel value ($d_{ij} = d_{ji}$ and $d_{ii} = 0$)

i = pixel i

j = pixel j

The distance matrix, where the d_{ij} is computed, can be built in different dimensions, allowing to consider more than one layer/band at time. If only one layer is considered, like in our case where a NDVI data-set was used, d_{ij} can be calculated as a simple Euclidean distance. If more layers are considered, d_{ij} can be computed relying for example on the Euclidean, Manhattan and Canberra distances (Rocchini et al., 2017). The formulas of such distances, with their advantages and disadvantages have been described by Rocchini et al. (2017) together with a straightforward R-package function (*spectralrao()*) to calculate the Q_{rs} in a single or multi-dimensional environment, allowing to calculate the Rao's Q with a moving window of different sizes. In our case we decided to implement the function to obtain a single value of Rao's Q for the whole plot area (100m x 100m in our case) representing our local landscape. This choice was made for an appropriate comparison with the data of species diversity that were collected at plot level.

The CV (formula 8) has been also widely used in different researches as SH index (Gholizadeh et al., 2018), (Levin et al., 2007) , and was calculated as:

$$CV = SD/\overline{x} \tag{8}$$

where:

CV = Coefficient of Variation

SD = Standard Deviation of NDVI for each plot image

$\overline{x}$ = mean of the NDVI value of each plot image

For each plot, the species diversity estimated through the Shannon's H derived from in-situ data and the spectral heterogeneity derived from the

two indices for the Sentinel-2 and Landsat 8 images were correlated by linear regression. The approach is summarized in Figure 2.

For all the twenty plots, a time-series of NDVI values for the available images was obtained (mean of the pixel of each plot) to understand the temporal variation within the year and the relation to the SVH.

3 Results

3.1 Sentinel-2

Figures 3 A and C (see also Table 1) show the temporal trend of the coefficient of determination (R^2) between Shannon's H derived from field data and two SH indices derived from the Sentinel-2 NDVI images for 2016 and 2017, respectively. Figures 3 B and D show the NDVI time-series as the mean NDVI value of all the twenty study areas for the year 2016 and 2017 respectively. The boxes show the 25th and 75th quantile, the dots represent the outliers (see Appendix 2 for all the sampling plot based NDVI time series). The R^2 of Rao's Q and CV had a similar trend, reaching the highest value between June and July (180^{th}-200^{th} day of the year) and decreasing towards winter and spring similarly to the NDVI time-series.

For both years, the Rao's Q index showed the highest relation, reaching values of R^2=0.48 and R^2=0.70 for the year 2016 and 2017, respectively (Table 1). The difference in R^2 between the two years was mainly related to a combined effect of missing images in 2016 (in particular during the peak of NDVI) due to cloudiness and the absence of the Sentinel-2 B satellite (available since July 2017).

3.2 Landsat 8

Figures 4 A and C (see also Table 2) show the temporal trend of the relation between the Shannon's H derived from field data and the two SH indices calculated from Landsat 8 NDVI images. The NDVI time-series, derived as the mean NDVI value of the twenty plots is shown in Figures 4 B and D for year 2016 and 2017, respectively (see Appendix 2 for all the related linear regressions). Also in this case, the relation between field-derived and remotely derived Rao's Q and CV had a similar trend of NDVI, reaching the highest R^2 value when the vegetation index is at its peak.

For both years, irrespective of the sensor, the Rao's Q index showed higher relation with field data in comparison with the CV (Figure 3). For 2017, the relation between field-derived Shannon's H and the indices calculated from

Landsat 8 images were lower than those resulting from Sentinel-2 images. On the contrary, no particular differences were observed between the two sensors in 2016. The regression model together with R^2 and p values for all the plots are shown in Appendix 2.

Since the analysis are based on testing multiple hypotheses, the p-values, used as a measure of significance, were corrected with the Benjamin-Hochberg correction (Benjamini and Hochberg , 1995). The corrected p-values confirm the strong relation between species and spectral diversity. In fact, the relation between the SH calculated with Rao's Q (for both Sentinel-2 and Landsat 8) and the field based Shannon's H were, near or at the NDVI peak period, always significant. The CV did not show the same level of significance, having for some years and sensors (e.g. Landsat 8 in 2017 and Sentinel-2 in 2016) high p-values (Appendix 2).

4 Discussion

In this paper the Spectral Hypothesis has been tested for the first time in an alpine coniferous forest to estimate the tree species diversity. We tested the goodness of the Rao's Q as a new SH index. Rao's Q showed higher correlation to field measurement than the widely used CV, since it directly accounts for both distance among pixel values as well as their relative abundance in a single formula. The CV showed similar results, with a trend similar to the Rao's Q index but with a lower level of relation compared to the Rao's Q. The CV has been used among the others by Wang et al. (Wang et al., 2018) showing that the relative contributions of richness, evenness, and composition to the spectral reflectance variability, in a hyperspectral data-set of a prairie ecosystem, could not be discriminated.

In our research, we also took in consideration the use of Shannon's H as SH index (Rocchini et al., 2017). We realized that this index cannot be used as a measure of spectral in an image with continuous (floating) values such as the NDVI. The pixel values cannot be treated as categories and it is highly unlikely that two pixels will have exactly the same value, thus the calculation result will only depend on the number of pixels considered. As an example having an image of four pixels with the following numbers: IMG1(1, 7, 8 , 10) will lead to the same Shannon's value of an image having the following numbers: IMG2(1, 10, 100, 200), since every value occupies the same area (25%) of the image. In both cases, Shannon's H would be 1.386294. On the contrary Rao's Q takes into account the distance among values besides their relative abundance, reaching a value of 3.5 for IMG1 and a value of 85.9 for

IMG2.

This paper highlighted the importance of a time-series approach in testing the SVH. Our results showed that the relation between field data and all the SH indices vary strongly within the year. In 2017 for the Rao's Q index, minimum values are generally found in winter (R^2=0.16) while maximum values are reached in summer (R^2=0.7) when the NDVI reached its peak. Previous studies focused primarily just on a specific period of the year and obtaining in general lower level of relationship. Rocchini et al. (Rocchini, 2007) for example tested the SVH to estimate the species richness of a wetland ecosystem in Central Italy using a single image of June 2002 reaching a R^2 value of 0.48. Madonsela et al. (Madonsela et al., 2017) compared data of alpha diversity from the Savannah woodland in southern Africa with the spectral variability of single bands and different vegetation indices derived from three Landsat 8 images in March 2016 (end of the wet season), reaching a maximum R^2 value of 0.41.

Our results support one of the main outcomes of a study previously carried out by Schmidtlein and Fassnacht (2017), who underlined that the relation between spectral variability and species is season-dependent. Also Feilhauer and Schmidtlein (2011) showed that the relation between species composition and reflectance changes over time, with the highest correlation near the vegetation optimum. In this paper, a significant relationship between tree species diversity and the SH of NDVI was shown, particularly when the vegetation index reached the highest seasonal values. This is due to the fact that, when NDVI reaches its highest values, it is able to capture small variation in reflectance of different leaf traits typical of specific trees (He et al., 2009). According to Parviainen et al. (2010), species richness, related to the habitat heterogeneity is reflected by the variability of NDVI. Our study was not the first attempt to test the SVH with NDVI data, previous studies tested it, without using a multi-temporal approach: Levin et al. (2007) tested the spectral variation of NDVI images derived from Landsat 7 (ETM +), Aster and QuickBird to examine the relationship with plant richness and rarity in Mediterranean forests. Gillespie (2005) predicted the richness of woody-plant species in a tropical dry forest, testing the SVH with a single image of NDVI derived from a Landsat 7 (ETM +) image. The variation of three NDVI images, derived from Landsat 8, has been used by Madonsela et al. (2017) to quantify tree species diversity in Savannah woodland.

This research confirmed that the SVH is scale and sensor dependent: a decrease in spatial resolution influences the spectral heterogeneity creating

mixed pixels that can threaten the ability of matching spectral heterogeneity with field heterogeneity. Sentinel-2 data showed better results testing the SVH due to its high-intermediate spatial resolution (10m) peculiar to discriminate forest trees. The quick revisit time of the new European satellite (5 days at equator with both the Sentinel-2 A and B) gives also the possibility to acquire several images per year, particularly important for the study of the SVH in alpine regions, where the meteorological conditions (for example clouds, haze, snow, topographic effects) are not always optimal. Focusing on the Sentinel-2 results, the difference in R^2 between 2016 and 2017 was evident, underlying the importance of the number of available images for the application of SVH.

Concerns may arise about the approach that we used: the Sentinel-2 data could have been re-scaled to 30 meter resolution without using the Landsat-8 satellite but, as underlined by Rahbek (2005), the spectral variability depends on the scene and on the sensors; research that deal with the effects of spatial and spectral resolution should not ignore these two important aspects.

In this study, the effect of the grain size of sampling units in the study area has not been investigated. The grain effect on the link between SH and species diversity have been examined by different authors: Rocchini et al. (Rocchini et al., 2004), applying the SVH to a wetland ecosystem found out that, the increase of the spatial scale of analysis (from $100m^2$ to 1ha) brings to a higher correlation between spectral heterogeneity and species richness. Similar results were obtained by Oldeland et al. (2010) who estimated vegetation species diversity in Central Namibia, finding that correlation improves while increasing the window of analysis (from $100m^2$ to $1000m^2$). This issue called Modifiable Areal Unit Problem (MAUP) that involves many studies of landscape ecology has been well discussed and analyzed by Jelinski and Wu (Jelinski and Wu, 1996). From our side, it was very difficult to study this effect, in particular with the Landsat 8 data that, with a lower resolution (30m) does not allow to test the SVH in smaller areas (already limited using nine pixel).

An additional concern that may emerge could deal with the small extent of the study area, a dense alpine coniferous forest dominated mainly by pines, larches and spruces. Other studies tested the SVH in relative small areas, considering a limited number of plots. Gould et al. (2000) tested the SVH in the Hood river region of the central Canadian arctic using 17 plots of $0.5km^2$ size. Rocchini et al. (Rocchini et al., 2004) used 22 plots to test the spectral variation of multispectral images for the estimation of the species diversity in a wetland area in Central Italy. This study represents a first step to understand the relation between the spectral variability and the species diversity in an alpine coniferous forest, since no similar studies have been carried out in

this ecosystem to date. This point represents a typical bias of any empirical study and the results of this research can probably be applicable to wider areas on the strength of the general relation between SH and species diversity (Rocchini, 2007). As stressed in the introduction, the SVH is not based on catching directly species diversity in the field, but on using indirect measures based on environmental heterogeneity. The spectral variability of a remotely sensed image can be directly related to environmental heterogeneity which in turn might be a proxy of species diversity. Yet the biodiversity of a certain ecosystem is affected by much more than environmental heterogeneity alone; however, as we stated in our objectives, the main aim of this paper was to test the reliability of the SVH as a proxy for tree species diversity in a coniferous forest ecosystem.

5 Conclusion

This study has focused on the relation between tree species diversity and spectral variation of a multi-temporal NDVI time-series, derived from Sentinel-2 and Landsat 8 satellites, in an alpine coniferous forest ecosystem. The SVH has been tested with the new SH index Rao's Q and compared with the CV, a well known SH index. The Rao's Q performed better than the CV index, particularly the Sentinel-2 data. This research underlined the relevance of the NDVI in the study of the SVH, therefore proving the importance of the multi-temporal approach.

As we stressed in the introduction, in the past decades, the SVH has been tested in different ecosystems, with various remote sensing optical data, using several new SH indices reaching in general discrete to positive results similar to those of this research. While the approach being proposed has successfully led to a clear relationship between spectral and field diversity, we are aware that further tests should be conducted in different environments before the approach can be considered as a generalizable method, as also pointed out by Schmidtlein and Fassnacht (2017).

The study of species diversity through remote sensing data in complex landscapes such as the Alps and alpine habitats, like the coniferous forests considered in this study, gives the opportunity to rapidly estimate biodiversity in highly topographically complex regions to further potentially guide field sampling. The results of this research, can be used in a practical way as a "first filter" in the localization of biodiversity hotspots (Rocchini, 2007) or in the prediction of spatial changes over time.

6 Acknowledgements

We are grateful to the Editor and to two anonymous reviewers who provided useful insights on a previous version of the manuscript. DR and RS were supported by the H2020 project ECOPOTENTIAL (grant agreement 641762). DR was supported by the H2020 TRuStEE - Training on Remote Sensing for Ecosystem Modelling project (grant agreement 721995).

References

Bellard, C., Bertelsmeier, C., Leadley, P., Thuiller, W., Courchamp, F. (2012). Impacts of climate change on the future of biodiversity. Ecology Letters, 15: 365-377.

Benjamini, Y., Hochberg, Y. (1995). Controlling the false discovery rate: a practical and powerful approach to multiple testing. Journal of the Royal statistical society: series B (Methodological), 57:289-300.

Bergen, K., Goetz, S., Dubayah, R., Henebry, G., Hunsaker, C., Imhoff, M., Nelson, R., Parker, G., Radeloff, V. (2009). Remote sensing of vegetation 3-D structure for biodiversity and habitat: review and implications for lidar and radar spaceborne missions. Journal of Geophysical Research: Biogeosciences, 114.

Bhardwaj, A., Joshi, P.K., Sam, L., Singh, M.K., Singh, S., Kumar, R. (2015). Applicability of Landsat 8 data for characterizing glacier facies and supraglacial debris. International Journal of Applied Earth Observation and Geoinformation, 38: 51-64.

Botta-Dukat, Z. (2005). Rao's quadratic entropy as a measure of functional diversity based on multiple traits. Journal of Vegetation Science, 16: 533-540.

Carlson, K.M., Asner, G.P., Hughes, R.F., Ostertag, R., Martin, R.E. (2007). Hyperspectral remote sensing of canopy biodiversity in Hawaiian lowland rainforests. Ecosystems, 10: 536-549.

Chaudhary, A., Burivalova, Z., Koh, L.P., Hellweg, S. (2016). Impact of forest management on species richness: global meta-analysis and economic trade-offs. Scientific Reports, 6: 23954.

553 Chrysafis, I., Mallinis, G., Siachalou, S., Patias, P. (2017). Assessing the
554 relationships between growing stock volume and Sentinel-2 imagery in a
555 Mediterranean forest ecosystem. Remote Sensing Letters, 8: 508-517.

556 Cunningham, R. (1963). The effect of clearing a tropical forest soil. European
557 Journal of Soil Science, 14: 334-345.

558 Dandois, J.P., Olano, M., Ellis, E.C. (2015). Optimal altitude, overlap, and
559 weather conditions for computer vision UAV estimates of forest structure.
560 Remote Sensing, 7: 13895-13920.

561 Feilhauer, H., Schmidtlein, S. (2011). On variable relations between veg-
562 etation patterns and canopy reflectance. Ecological Informatics 2011, 6:
563 83-92.

564 Féret, J.B., Asner, G.P. (2014). Mapping tropical forest canopy diversity
565 using high-fidelity imaging spectroscopy. Ecological Applications, 24: 1289-
566 1296.

567 Fleming, R., Brown, N., Jenik, J., Kahumbu, P., Plesnik, J. (2011). Emerging
568 perspectives on forest biodiversity. UNEP Year Book 2011, pp. 47-59.

569 Gamfeldt, L., Hillebrand, H., Jonsson, P.R. (2008). Multiple functions in-
570 crease the importance of biodiversity for overall ecosystem functioning.
571 Ecology, 89: 1223-1231.

572 Garzon–Lopez, C. X., Bohlman, S.A., Olff, H., Jansen, P. A. (2013). Map-
573 ping tropical forest trees using high–resolution aerial digital photographs.
574 Biotropica, 43: 308-316.

575 Getzin, S., Wiegand, K., Schöning, I. (2012). Assessing biodiversity in forests
576 using very high–resolution images and unmanned aerial vehicles. Methods
577 in Ecology and Evolution, 3: 397-404.

578 Gholizadeh, H., Gamon, J.A., Zygielbaum, A.I., Wang, R., Schweiger, A.K.,
579 Cavender-Bares, J. (2018). Remote sensing of biodiversity: soil correc-
580 tion and data dimension reduction methods improve assessment of alpha-
581 diversity (species richness) in prairie ecosystems. Remote Sensing of Envi-
582 ronment, 206: 240-253.

583 Gillespie, T.W. (2005). Predicting woody-plant species richness in tropical
584 dry forests: a case study from South Florida, USA. Ecological Applications,
585 15: 27-37.

586 Gillespie, T.W., Foody, G.M., Rocchini, D., Giorgi, A.P., Saatchi, S. (2008).
587 Measuring and modelling biodiversity from space. Progress in Physical
588 Geography, 32: 203-221.

589 Gong, P., Pu, R., Yu, B. (1997). Conifer species recognition: An exploratory
590 analysis of in situ hyperspectral data. Remote sensing of Environment, 62:
591 189-200.

592 Gorelick, R. (2006). Combining richness and abundance into a single diver-
593 sity index using matrix analogues of Shannon's and Simpson's indices.
594 Ecography, 29: 525-530.

595 Gould, W. (2000). Remote sensing of vegetation, plant species richness, and
596 regional biodiversity hotspots. Ecological Applications, 10: 1861-1870.

597 Grote, R., Samson, R., Alonso, R., Amorim, J.H., CariÃśanos, P., Churkina,
598 G., Fares, S., Le Thiec, D., Niinemets, U., Mikkelsen, T.N., Paoletti, E.,
599 Tiwary, A., Calfapietra, C. (2016). Functional traits of urban trees: air
600 pollution mitigation potential. Frontiers in Ecology and the Environment,
601 14: 543-550.

602 Hall, K., Johansson, L., Sykes, M., Reitalu, T., Larsson, K., Prentice, H.C.
603 (2010). Inventorying management status and plant species richness in semi-
604 natural grasslands using high spatial resolution imagery. Applied Vegeta-
605 tion Science, 13: 221-233.

606 Hanski, I. (2011) Habitat loss, the dynamics of biodiversity, and a perspective
607 on conservation. Ambio, 40: 248-255.

608 He, K.S., Zhang, J., Zhang, Q. (2009). Linking variability in species com-
609 position and MODIS NDVI based on beta diversity measurements. Acta
610 Oecologica, 35: 14-21.

611 Kaennel, M. (1998). Biodiversity: a diversity in definition. In: Assessment of
612 biodiversity for improved forest planning, Springer, 1998, pp. 71-81.

613 Immitzer, M., Vuolo, F., Atzberger, C. (2016). First experience with Sentinel-
614 2 data for crop and tree species classifications in central Europe. Remote
615 Sensing, 8: 166.

616 Innes, J.L., Koch, B. (1998). Forest biodiversity and its assessment by remote
617 sensing. Global Ecology & Biogeography Letters, 7: 397-419.

618 Jelinski, D. E., Wu, J. (1996). The modifiable areal unit problem and impli-
619 cations for landscape ecology. Landscape ecology, 11(3), 129-140.

Jetz, W., Cavender-Bares, J., Pavlick, R., Schimel, D., Davis, F.W., Asner, G.P., Guralnick, R., Kattge, J., Latimer, A.M., Moorcroft, P., Schaepman, M.E., Schildhauer, M.P., Schneider, F.D., Schrodt, F., Stahl, U., Ustin, S.L. (2016). Monitoring plant functional diversity from space. Nature Plants, 2: 193.

Jung, K., Kaiser, S., BÃűhm, S., Nieschulze, J., Kalko, E.K. (2012). Moving in three dimensions: effects of structural complexity on occurrence and activity of insectivorous bats in managed forest stands. Journal of Applied Ecology, 49: 523-531.

Lassau, S.A., Cassis, G., Flemons, P.K., Wilkie, L., Hochuli, D.F. (2005) Using high-resolution multi-spectral imagery to estimate habitat complexity in open-canopy forests: can we predict ant community patterns? Ecography, 28: 495-504.

Laurin, G.V., Chan, J.C.W., Chen, Q., Lindsell, J.A., Coomes, D.A., Guerriero, L., Del Frate, F., Miglietta, F., Valentini, R. (2014). Biodiversity mapping in a tropical West African forest with airborne hyperspectral data. PLoS ONE, 9: e97910.

Legendre, P., Legendre, L. (1998). Numerical Ecology (second English ed.), Elsevier, Amsterdam, The Netherlands.

Levin, N., Shmida, A., Levanoni, O., Tamari, H., Kark, S. (2007). Predicting mountain plant richness and rarity from space using satellite-derived vegetation indices. Diversity and Distributions, 13: 692-703.

Lindenmayer, D., Franklin, J., Fischer, J. (2006). General management principles and a checklist of strategies to guide forest biodiversity conservation. Biological Conservation, 131: 433-445.

Lopes, M., Fauvel, M., Ouin, A., Girard, S. (2017). Spectro-temporal heterogeneity measures from dense high spatial resolution satellite image time series: Application to grassland species diversity estimation. Remote Sensing, 9: 993.

Madonsela, S., Cho, M.A., Ramoelo, A., Mutanga, O. (2017). Remote sensing of species diversity using Landsat 8 spectral variables. ISPRS Journal of Photogrammetry and Remote Sensing, 133: 116-127.

Mace, G.M., Norris, K., Fitter, A.H. (2012). Biodiversity and ecosystem services: a multilayered relationship. Trends in Ecology & Evolution, 27: 19-26.

McNeely, J.A. (1992). The sinking ark: pollution and the worldwide loss of biodiversity. Biodiversity and Conservation, 1: 2-18.

Muller, J., Brandl, R. (2009). Assessing biodiversity by remote sensing in mountainous terrain: the potential of LiDAR to predict forest beetle assemblages. Journal of Applied Ecology, 46: 897-905.

Muller, J., Vierling, K. (2014). Assessing biodiversity by airborne laser scanning. In: Forestry Applications of Airborne Laser Scanning, Springer, pp. 357-374.

Mura, M., Bottalico, F., Giannetti, F., Bertani, R., Giannini, R., Mancini, M., Orlandini, S., Travaglini, D., Chirici, G. (2018) Exploiting the capabilities of the Sentinel-2 multi spectral instrument for predicting growing stock volume in forest ecosystems. International Journal of Applied Earth Observation and Geoinformation, 66: 126-134.

Nagendra, H. (2001). Using remote sensing to assess biodiversity. International Journal of Remote Sensing, 22: 2377-2400.

Nagendra, H. (2002). Opposite trends in response for the Shannon and Simpson indices of landscape diversity. Applied Geography, 22: 175-186.

Nagendra, H., Rocchini, D. (2008). High resolution satellite imagery for tropical biodiversity studies: the devil is in the detail. Biodiversity and Conservation, 17: 3431.

Nagendra, H., Rocchini, D., Ghate, R., Sharma, B.„ Pareeth, S. (2010). Assessing plant diversity in a dry tropical forest: comparing the utility of Landsat and IKONOS satellite images. Remote Sensing, 2: 478-496.

Oindo, B.O., Skidmore, A.K. (2002). Interannual variability of NDVI and species richness in Kenya. International Journal of Remote Sensing, 23: 285-298.

Oldeland, J., Wesuls, D., Rocchini, D., Schmidt, M., Jurgens, N. (2010). Does using species abundance data improve estimates of species diversity from remotely sensed spectral heterogeneity? Ecological Indicators, 10: 390-396.

Palmer, M.W., Earls, P.G., Hoagland, B.W., White, P.S., Wohlgemuth, T. (2002). Quantitative tools for perfecting species lists. Environmetrics, 13: 121-137.

Parviainen, M., Luoto, M., Heikkinen, R.K. (2010). NDVI-based productivity and heterogeneity as indicators of plant-species richness in boreal landscapes. Boreal Environment Research, 15: 301-318.

Podani, J. (2000). Introduction to the exploration of multivariate biological data, Backhuys Publishers, Kerkwerve, The Netherlands.

Puletti, N., Chianucci, F., Castaldi, C. (2017) Use of Sentinel-2 for forest classification in Mediterranean environments. Annals of Silvicultural Research, 42.

Rahbek, C. (2005). The role of spatial scale and the perception of large-scale species-richness patterns. Ecology Letters, 8: 224-239.

Rao, C.R. (1982). Diversity and dissimilarity coefficients: a unified approach. Theoretical Population Biology, 21: 24-43.

Rocchini, D. (2007). Effects of spatial and spectral resolution in estimating ecosystem α diversity by satellite imagery. Remote Sensing of Environment, 111: 423-434.

Rocchini, D., Balkenhol, N., Carter, G.A., Foody, G.M. Gillespie, T.W., He, K.S., Kark, S., Levin, N., Lucas, K., Luoto, M., Nagendra, H., Oldeland, J., Ricotta, C., Southworth, J., Neteler, M. (2010). Remotely sensed spectral heterogeneity as a proxy of species diversity: recent advances and open challenges. Ecological Informatics, 5: 318-329.

Rocchini, D., Chiarucci, A., Loiselle, S.A. (2004). Testing the spectral variation hypothesis by using satellite multispectral images. Acta Oecologica, 26: 117-120.

Rocchini, D., Luque, S., Pettorelli, N., Bastin, L., Doktor, D., Faedi, N., Feilhauer, H., Féret, J.-B., Foody, G.M., Gavish, Y., Godinho, S., Kunin, W.E., Lausch, A., Leitao, P.J., Marcantonio, M., Neteler, M., Ricotta, C., Schmidtlein, S., Vihervaara, P., Wegmann, M., Nagendra, H. (2018). Measuring β-diversity by remote sensing: a challenge for biodiversity monitoring. Methods in Ecology and Evolution, 9: 1787-1798.

Rocchini, D., Marcantonio, M., Ricotta, C. (2017). Measuring Rao's Q diversity index from remote sensing: An open source solution. Ecological Indicators, 72: 234-238.

Rocchini, D.; Neteler, M. (2017). Spectral rank-abundance for measuring landscape diversity. International journal of remote sensing 2012, 33, 4458-4470.

Schmidtlein, S., Fassnacht, F.E. (2017). The spectral variability hypothesis does not hold across landscapes. Remote Sensing of Environment, 192: 114-125.

Schneider, F. D., Morsdorf, F., Schmid, B., Petchey, O. L., Hueni, A., Schimel, D. S., Schaepman, M. E. (2017). Mapping functional diversity from remotely sensed morphological and physiological forest traits. Nature communications, 8(1):1441.

Sepkoski, J.J. (1988). Alpha, beta, or gamma: where does all the diversity go? Paleobiology, 14: 221-234.

Shannon, C. (1948). A mathematical theory of communication, Bell System Technology Journal, 27: 379-423.

Simonson, W.D., Allen, H.D., Coomes, D.A. (2012). Use of an airborne lidar system to model plant species composition and diversity of Mediterranean oak forests. Conservation Biology, 26: 840-850.

Team, C.W., Pachauri, R., Reisinger, A. (2007). Contribution of working groups I, II and III to the fourth assessment report of the intergovernmental panel on climate change. IPCC, Geneva, Switzerland 2007.

Turner, W., Spector, S., Gardiner, N., Fladeland, M., Sterling, E., Steininger, M. (2003). Remote sensing for biodiversity science and conservation. Trends in Ecology & Evolution, 18: 306-314.

Tucker, C. J. (1979). Red and photographic infrared linear combinations for monitoring vegetation. Remote sensing of Environment, 8(2), 127-150.

Verhegghen, A., Eva, H., Ceccherini, G., Achard, F., Gond, V., Gourlet-Fleury, S., Cerutti, P.O. (2016). The potential of Sentinel satellites for burnt area mapping and monitoring in the Congo Basin forests. Remote Sensing, 8: 986.

Wang, R., Gamon, J.A., Schweiger, A.K., Cavender-Bares, J., Townsend, P.A., Zygielbaum, A.I., Kothari, S. (2018). Influence of species richness, evenness, and composition on optical diversity: A simulation study. Remote Sensing of Environment, 211: 218-228.

White, J.C., Gomez, C., Wulder, M.A., Coops, N.C. (2010). Characterizing temperate forest structural and spectral diversity with Hyperion EO-1 data. Remote Sensing of Environment, 114: 1576-1589.

Whittaker, R.H. (1960). Vegetation of the Siskiyou mountains, Oregon and California. Ecological monographs, 30: 279-338.

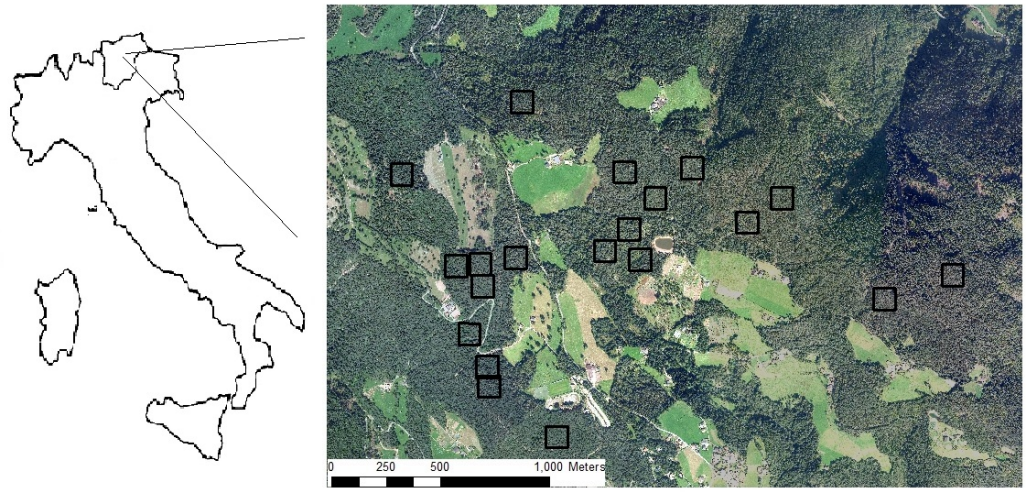

Figure 1: The study area located in the municipality of San Genesio-Jenesien (South Tyrol) Italy. The 20 plots are indicated by black squares.

Table 1: R^2 derived from the linear regression between the two SH indices (Rao's Q and CV) and the species diversity (Shannon's H field based) for the Sentinel-2 images. The higher relation values for each year and SH index are in bold.

	Date	Rao's Q	CV
	03.20	0.23	0.18
	04.12	0.40	0.37
	05.22	0.27	0.22
	06.22	**0.47**	**0.35**
	07.18	0.42	0.32
	08.27	0.32	0.26
2016	**09.06**	0.36	0.31
	09.09	0.26	0.23
	09.26	0.29	0.23
	10.16	0.27	0.19
	10.29	0.31	0.27
	12.15	0.31	0.19
	01.07	0.34	0.25
	02.16	0.36	0.33
	03.25	0.35	0.31
	03.28	0.36	0.33
	04.14	0.16	0.14
	05.17	0.15	0.09
	05.27	0.37	0.25
	06.13	**0.7**	**0.61**
	06.26	0.61	0.54
2017	**07.06**	0.61	0.56
	07.08	0.56	0.52
	07.18	0.62	0.56
	08.07	0.62	0.57
	08.22	0.5	0.45
	08.30	0.59	0.55
	09.21	0.43	0.36
	10.09	0.24	0.2
	10.16	0.22	0.16
	10.24	0.36	0.31
	11.15	0.43	0.35
	12.15	0.27	0.18

Table 2: R^2 derived from the linear regression between the two SH indices (Rao's Q and CV) and the species diversity (Shannon's H field based) for the Landsat 8 images. The higher relation values for each year and SH index are in bold.

	Date	Rao's Q	CV
	02.24	0.05	0.04
	03.20	0	0.01
	04.12	0.06	0.06
	05.07	0.07	0.06
	06.24	**0.48**	**0.37**
	07.10	0.31	0.27
2016	**07.17**	0.27	0.23
	09.12	0.14	0.11
	10.05	0.04	0.03
	10.23	0.11	0.1
	10.30	0.12	0.1
	11.15	0	0.01
	12.08	0.06	0.05
	12.17	0.02	0.04
	01.02	0.02	0.03
	01.18	0.16	0.13
	01.25	0.05	0.06
	03.14	0.16	0.15
2017	**04.08**	0.11	0.11
	05.17	0.11	0.06
	05.26	0.25	0.2
	06.11	0.32	0.25
	06.18	**0.42**	**0.35**
	07.04	0.38	0.34
	08.05	0.3	0.26
	08.30	0.21	0.18
	09.22	0.13	0.1
	11.18	0.15	0.13
	12.04	0.12	0.1
	12.20	0.01	0.03

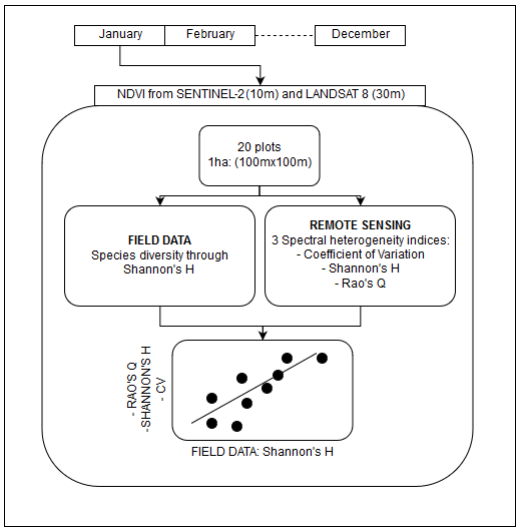

Figure 2: Flowchart representing the approach we used in this study: the linear regressions between field data and remote sensing data were calculated for both sensors (Sentinel-2 and Landsat 8) for the NDVI time-series (2016 and 2017), using two different spectral heterogeneity indices.

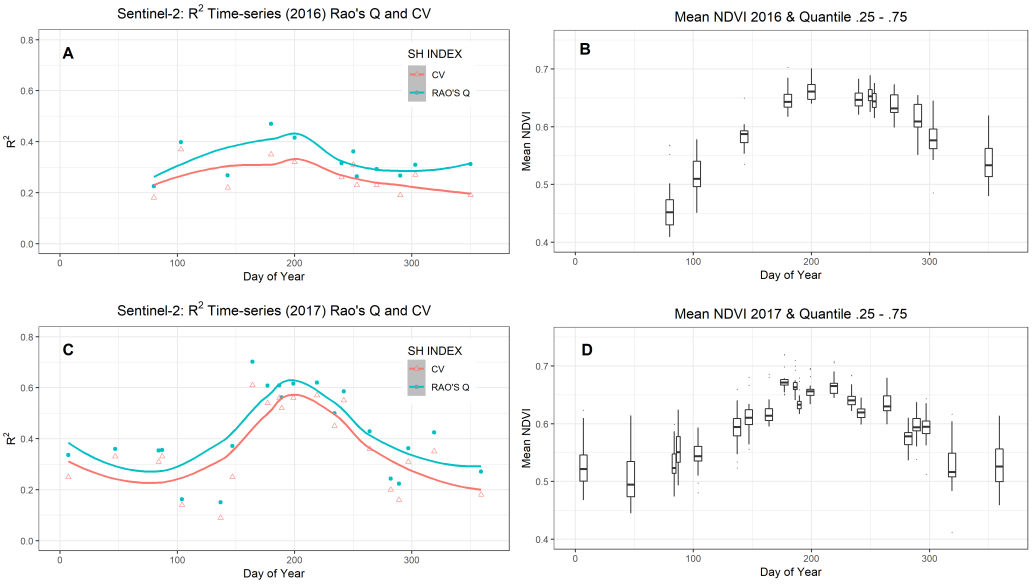

Figure 3: Sentinel-2: figures A and C show the time-series of the determination coefficient (R^2) between the field-based Shannon's H and the SH indices for the year 2016 and 2017 respectively. Points indicate the R^2 for the considered day. The line represent the smooth local regressions between the points. Figures B and D show the time-series statistics of mean NDVI value of all the study areas for both years. The boxes show the 25th and 75th quantile, the dots represent the out layers. The single relations for all the points and the NDVI time-series of the other areas are in the Appendix 2 of this paper.

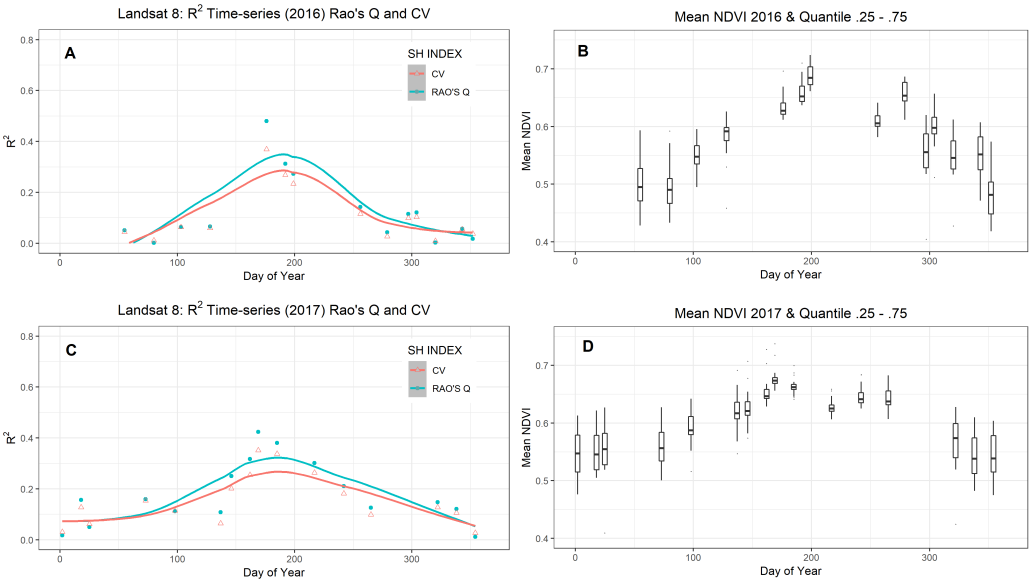

Figure 4: Landsat 8: figures A and C show the time-series of the determination coefficient (R^2) between the field-based Shannon's H and the SH indices for the year 2016 and 2017 respectively. Points indicate the R^2 for the considered day. The line represent the smooth local regressions between the points. Figures B and D show the time-series statistics of mean NDVI value of all the study areas for both the years. The boxes show the 25th and 75th quantile, the dots represent the out layers. The single relations for all the points and the NDVI time-series of the other areas are in the Appendix 2 of this paper.